NEOPLASIA
www.neoplasia.com

Volume 11 Number 5 May 2009 pp. 497–508 497

Cancer–Stellate Cell Interactions Perpetuate the Hypoxia-Fibrosis Cycle in Pancreatic Ductal Adenocarcinoma[1]

Mert Erkan[*,2], Carolin Reiser-Erkan[*,2], Christoph W. Michalski[*], Stefanie Deucker[*], Danguole Sauliunaite[*], Sylvia Streit[*], Irene Esposito[†,‡], Helmut Friess[*] and Jörg Kleeff[*,§]

[*]Department of General Surgery, Technische Universität München, Munich, Germany; [†]Institute of Pathology, Technische Universität München, Munich, Germany; [‡]Institute of Pathology, Helmholtz Zentrum München, Oberschleissheim, Germany; [§]Center of Cancer Systems Biology, Dept. of Medicine, Caritas St. Elizabeth's Medical Center, Tufts University School of Medicine, Boston, MA 02135-2997, USA

Abstract

BACKGROUND AND AIMS: Although both cancer and stellate cells (PSCs) secrete proangiogenic factors, pancreatic cancer is a scirrhous and hypoxic tumor. The impact of cancer-PSCs interactions on angiogenesis was analyzed. *METHODS:* Expression of periostin, CD31, and α-smooth muscle actin was assessed by immunohistochemistry. Human PSCs and cancer cells were cultivated under normoxia and hypoxia alone, or in coculture, to analyze the changes in their angiogenic and fibrogenic attributes, using enzyme-linked immunosorbent assay, immunoblot, and quantitative polymerase chain reaction analyses and growth of cultured endothelial cells *in vitro*. *RESULTS:* On the invasive front of the activated stroma, PSCs deposited a periostin-rich matrix around the capillaries in the periacinar spaces. Compared with the normal pancreas, there was a significant reduction in the microvessel density in chronic pancreatitis (five-fold, $P < .001$) and pancreatic cancer (four-fold, $P < .01$) tissues. *In vitro*, hypoxia increased PSCs' activity and doubled the secretion of periostin, type I collagen, fibronectin, and vascular endothelial growth factor (VEGF). Cancer cells induced VEGF secretion of PSCs (390 ± 60%, $P < .001$), whereas PSCs increased the endostatin production of cancer cells (210 ± 14%, $P < .001$) by matrix metalloproteinase–dependent cleavage. *In vitro*, PSCs increased the endothelial cell growth, whereas cancer cells alone, or their coculture with PSCs, suppressed it. *CONCLUSIONS:* Although PSCs are the dominant producers of VEGF and increase endothelial cell growth *in vitro*, in the peritumoral stroma, they contribute to the fibrotic/hypoxic milieu through abnormal extracellular matrix deposition and by amplifying endostatin production of cancer cells.

Neoplasia (2009) 11, 497–508

Abbreviations: CL, cell lysate; CP, chronic pancreatitis; ECM, extracellular matrix; PCC, pancreatic cancer cell; PDAC, pancreatic ductal adenocarcinoma; PSC, pancreatic stellate cell; SN, supernatant

Address all correspondence to: Jörg Kleeff, MD, Department of General Surgery, Technische Universität München, Klinikum rechts der Isar, 81675 Munich, Germany.
E-mail: kleeff@gmx.de

[1]This study was supported by a grant (Integrierten Verbunds der medizinischen Genomforschung, NGFN-Plus) from the German Federal Ministry of Education and Research (Bundesministerium für Bildung und Forschung – BMBF) grant number: 016S08115.
Competing interests: None declared.

[2]These authors contributed equally to this manuscript.

Received 17 December 2008; Revised 27 February 2009; Accepted 2 March 2009

DOI 10.1593/neo.81618

Introduction

The activated stroma of pancreatic cancer is an important feature of pancreatic ductal adenocarcinoma (PDAC) and has a significant impact on patient survival [1]. Pancreatic stellate cells (PSCs) produce this fibrotic/hypoxic microenvironment in which PDAC cells evolve [2–5]. Angiogenesis is essential for the growth and survival of solid tumors [6–8]. Without accompanying neoangiogenesis, tumors cannot exceed 1 to 2 mm in diameter [6–8]. According to standard reasoning, primary epithelial tumors that are initially separated from underlying vessels by the basement membrane eventually become hypoxic as they outgrow the ambient vascular supply [9,10]. Several artificial models in which tumor cells are seeded into initially avascular spaces (i.e., subcutaneous, cornea pocket, vitreous) prove that hypoxic tumor cells induce angiogenic in-growth by secretion of neoangiogenic substances such as vascular endothelial growth factor (VEGF) and angiopoietin 2 [10,11]. Such manipulation of the microenvironment allows further growth of the initial tumor [10,12,13]. However, recent evidence suggests that early on, tumor cells grow by co-opting existing host vessels; thus they start as well-vascularized tumors but later become hypoxic because of a defensive host response [10,14].

The production of a fibronectin- and type I collagen–rich extracellular matrix (ECM) is a crucial step in initiation of tumor angiogenesis [15–18]. Therefore, the early tumor microenvironments is associated with more stromal cells, enhanced capillary density, and type I collagen and fibrin deposition [4,13,15,19]. Although tumor cells can secrete VEGF themselves, stromal and inflammatory cells are the principal sources of host-derived VEGF [18,20].

We and others have previously shown that 1) the fibrotic stroma of the diseased pancreas is hypoxic [5,21], 2) pancreatic cancer cells (PCCs) and PSCs respond to tissue hypoxia with a robust hypoxia-inducible factor 1α protein increase [5,21], and 3) PSCs produce potent angiogenic substances such as VEGF, basic fibroblast growth factor, and periostin [3,4,22]. Therefore, it is difficult to explain why PDAC in humans is so scirrhous, with tissue oxygen tension remaining considerably lower than in the surrounding normal pancreas [5,21]. It also seems plausible that this already hypovascular microenvironment may be a reason that antiangiogenic therapies generally fail in PDAC [23].

In this study, we evaluated the fibrogenic and angiogenic responses of PSCs under hypoxia. To verify our *ex vivo* observations and *in vitro* results at a functional level, we used various models of pancreatic cancer and stellate cell cocultures to assess their individual and combined effects on the growth of endothelial cells.

Materials and Methods

Pancreatic Tissues and Human PSCs Cultivation

Tissue collection and preservation were performed as described previously [24]. Human PSCs were isolated from fibrotic areas of resected PDAC tissues using the outgrowth method, as described initially by Bachem et al. [3]. The use of human material for the analysis was approved by the local ethics committee of the University of Heidelberg, Germany, and written informed consent was obtained from all patients.

Human PCC Lines

Colo-357, MiaPaCa-2, Panc-1, and SU86.86 were either purchased from ATCC (Rockville, MD) or received as a kind gift from Dr. R. S. Metzgar (Durham, NC). The cells were routinely grown in complete medium (RPMI-1640 supplemented with 10% fetal bovine serum, 100 U/ml penicillin, and 100 μg/ml streptomycin) at 37°C and saturated with 5% CO_2 in a humid atmosphere.

Immunohistochemistry

Initial hematoxylin + eosin staining was performed to choose tissue blocks that contained large-enough areas of stroma for further immunohistochemical analysis. Immunohistochemistry (IHC) and quantitative color analysis were performed as described previously [1,4]. In brief, consecutive sections of normal pancreas (n = 5), chronic pancreatitis (CP; n = 20), and PDAC (n = 30) tissues were stained with α-smooth muscle actin (α-SMA; for PSCs, diluted 1:1500; M0851; DAKO Cytomation, Hamburg, Germany) and CD31 (for endothelial cells, diluted 1:50; M0823; DAKO Cytomation) without counterstaining to yield better quantification of the MVD. A frame of 4 × 4 mm was marked over the fibrotic area for analysis. Stromal tissue confined within this frame was then scanned automatically (mean area evaluated, 14 mm^2/section; mean number of 200× magnified fields: 90 per section). Image analysis was carried out using a Zeiss Axiocam 3.1 system and the KS300 3.0 program to evaluate the amount of PSCs and endothelial cell staining (Zeiss, Jena, Germany). The results were expressed as percent area positive for CD31/α-SMA in the total scanned surface. In representative blocks, immunohistochemical analysis was repeated with antiperiostin (1:4000, RD181045050; Biovendor, Heidelberg, Germany), α-SMA, and CD31 antibodies for demonstrative pictures.

Immunoblot Analysis and Densitometry

Immunoblot analyses of the cell lysates (CLs; for synthesis) and matching supernatants (SNs for secretion) as well as densitometric analysis of the blots were performed as described previously [4]. To demonstrate the interplay between PSCs activity (α-SMA), periostin, type I collagen, fibronectin synthesis, and secretion, each membrane was stripped and reblotted consecutively with the specific antibodies. γ-Tubulin was used to verify equal loading. Antibodies used: type Ia collagen (1:2000; sc-28657; Santa Cruz Biotechnology, Santa Cruz, CA), fibronectin (1:10,000; F3648; Sigma Aldrich, Taufkirchen, Germany), periostin (1:5000; RD181045050; Biovendor), α-SMA (1:10,000; M0851; DAKO Cytomation), matrix metalloproteinase 12 (MMP-12) antibody (AB19051) and positive control (AG902; Millipore, Schwalbach, Germany), and γ-tubulin (1:5000; sc-7396; Santa Cruz Biotechnology). Experiments were repeated three times using different PSC clones.

Collection of SNs and Enzyme-Linked Immunosorbent Assay

Cells were seeded in six-well plates (PSCs: 200,000 cells per well, PCCs: 400,000 cells per well) using the appropriate medium, i.e., RPMI-1640 with 10% fetal calf serum for PCCs, and stellate cell medium (1:1 [vol/vol] mixture of Dulbecco's modified Eagle medium and Ham's F12 medium with penicillin 1%, streptomycin 1%, and 10% fetal calf serum) for PSCs. Thereafter, all types of cells were incubated with serum-free stellate cell medium for the indicated periods. Five types of SNs were produced from sister clones of cells under both normoxic and hypoxic conditions: 1) Supernatants of PCC lines (Colo-357, MiaPaCa-2, Panc-1, and SU86.86); 2) Supernatants of PSCs; 3) Combined SNs of the coculture of PSCs at the bottom of a six-well

plate and Colo357, MiaPaCa-2, Panc-1, or SU86.86 in the insert of a coculture system (1 μm pore size; 352102; BD Falcon, Erembodegem, Belgium). Moreover, two types of exchange SNs were created using PSCs and PCCs in six-well plates. After 24 hours, the SNs were removed and used to incubate the reciprocal cells for another 24 hours; 4) Supernatant of PSCs that was subsequently used to incubate PCCs; 5) Supernatant of PCCs that was subsequently used to incubate PSCs. Each experiment was repeated at least three times using different PCC and PSC clones. All SNs were immediately centrifuged, aliquoted, frozen, and stored at −80°C until use. For the analyses, the following ELISA kits were used: VEGF (DVE00), endostatin (DNST0), and ProCathepsin B (DCATB0), all from R&D Systems, Wiesbaden-Nordenstadt, Germany.

Cultivation and Use of Primary Human Umbilical Vein Endothelial Cells

Cells were purchased and cultivated according to the manufacturer's recommendations (HUVEC-p C-12250; Promocell, Heidelberg, Germany). Five thousand cells were seeded in 100 μl of endothelial cell growth medium (C-22010; Promocell) supplemented with SupplementMix (C-39215; Promocell) in 96-well plates. Twenty-four hours later, 100 μl of appropriate SN was added to the cells. Forty-eight hours later, cell growth was analyzed by MTT assay as described previously [24]. Experiments were repeated at least four times in different combinations using two different human umbilical vein endothelial cells (HUVECs) and two different PSC clones.

Induction of Hypoxia

Sister clones of cancer cells and PSCs were kept under a hypoxic gas mixture (0.75% O_2, 10% CO_2, 89.25% N_2) for the indicated periods as described previously [5,24].

Inhibition of MMPs and Cathepsins B, S, and L

Because no specific MMP-12 inhibitor is commercially available, a broad-spectrum small-molecule MMP inhibitor (50 μM; ONO4817; Tocris, Bristol, UK), which also inhibits MMP-12, was used in cell culture experiments. For the inhibition of cathepsins, a broad-spectrum cathepsin inhibitor was used (10 μM; Z-FG-NHO-BzME; Merck, Whitehouse Station, NJ). DMSO was used as negative control.

Quantitative Polymerase Chain Reaction Analysis of Collagen XVIII Messenger RNA Expression

To analyze the regulation of collagen XVIII expression, total RNA from PSCs and PCCs were isolated using the RNeasy Mini Kit (Qiagen, Hilden, Germany) according to the manufacturer's instructions. Complementary DNA was generated from total RNA using the QuantiTect Reverse Transcription Kit (Qiagen) with 1 μg of RNA as a template. Quantitative gene expression was analyzed using the predesigned TaqMan Gene Expression Assay for Collagen XVIII (assay ID HS01043433_g1; containing two gene-specific primers and the probe mix solution) on a 7300 Real-Time PCR System (Applied Biosystems, Foster City, CA). Polymerase chain reactions were performed in duplicate, using *β-actin* as a housekeeping gene. The data

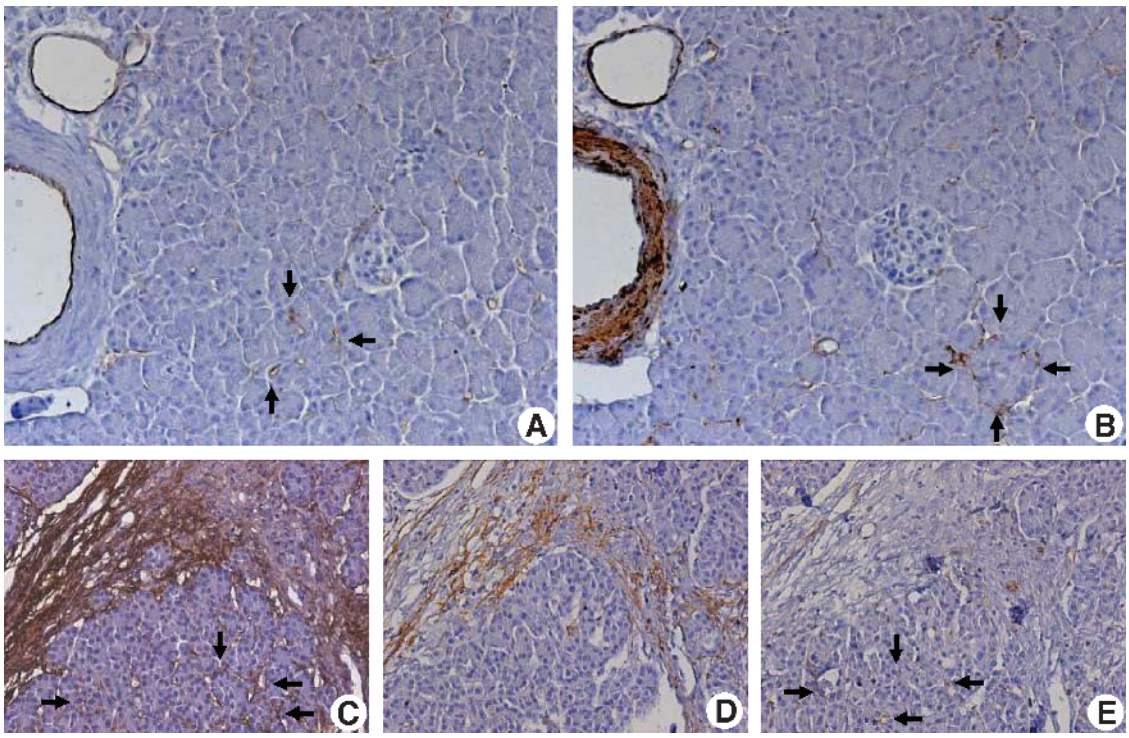

Figure 1. Localization of CD31, α-SMA, and periostin in normal and diseased pancreatic tissues: Immunohistochemical analysis was carried out using consecutive tissue sections of the normal pancreas. Sections were probed with antibodies against CD31 (A; original magnification, ×200) for endothelial cells and against α-SMA (B) for smooth muscle cells and PSCs. Analysis of periostin expression in CP tissues (C–E; original magnification, ×100): The PSCs in the periacinar spaces are marked by their periostin expression (C, arrows). Note that periostin-positive PSCs do not yet express α-SMA (D), and periostin has not yet been deposited in the periacinar spaces, where CD31-positive vessels are seen (E, arrows).

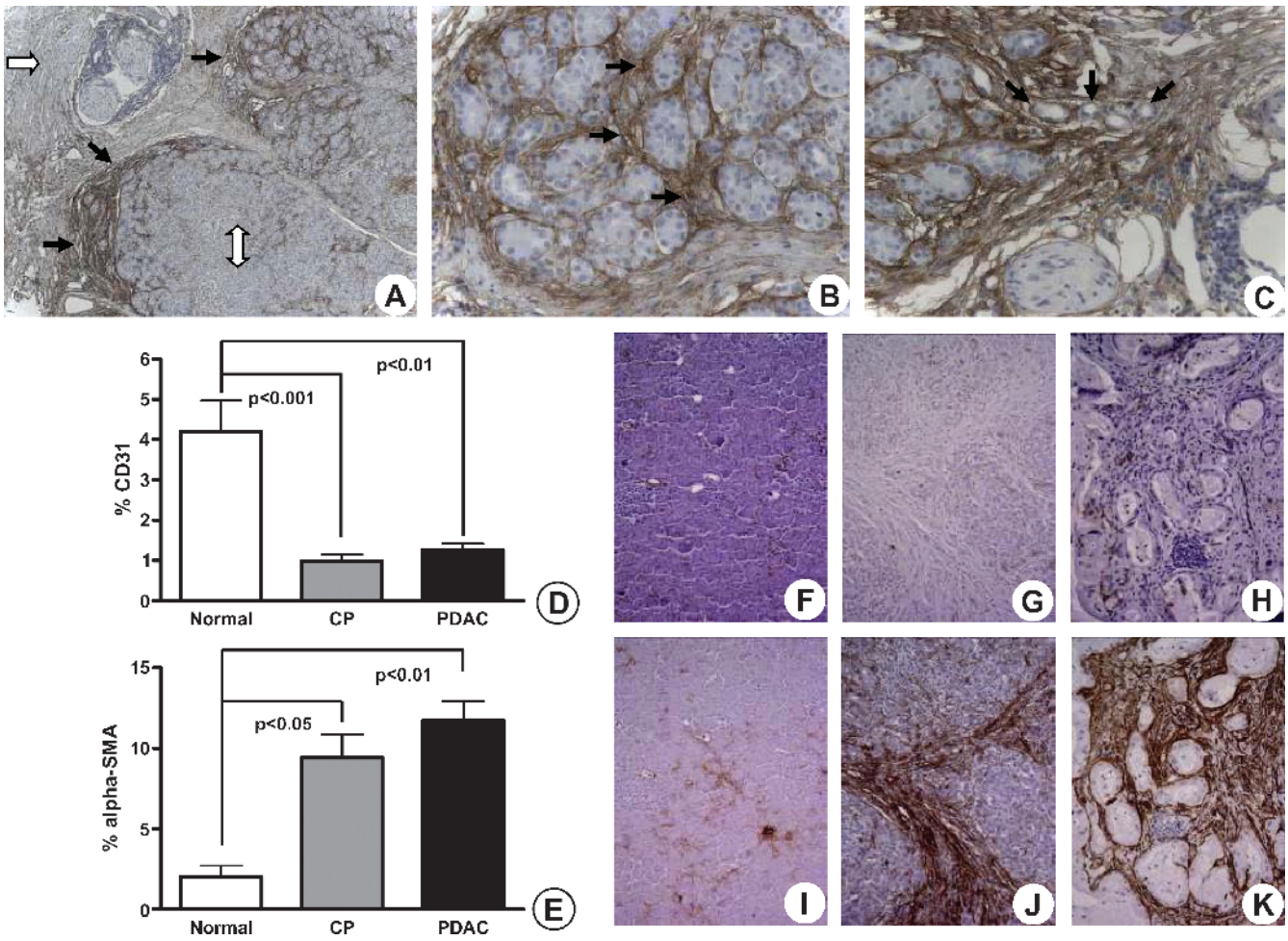

Figure 2. Site-specific deposition of periostin-rich stroma on the invasive front of the activated stroma in PDAC parallels increased α-SMA expression of PSCs and decreased vascularity in the diseased pancreas. Compared with both normal parenchyma (A; original magnification, ×50; white double-headed arrow) and organized ECM (white arrow), periostin expression dramatically increased at the interface where the activated stroma bordered on normal acini. The activation of stromal cells and detection of periostin expression in the CP-like changes surrounding the cancer occur even in areas where no cancer cells are visible. Although some periostin staining was detected in the interlobar septa (B and C; original magnification, ×200), the strongest expression was detected in the periacinar spaces (B, arrows). Notice the encasement of acini by the periostin-rich ECM and emergence of tubular complexes (C, arrows; original magnification, ×200). The percentage of CD31 (D) and α-SMA (E) staining in normal pancreas, CP, and PDAC tissues is graphically depicted. Results are expressed as mean ± SEM. Evaluation of CD31 (F, G, H) and α-SMA (I, J, K) using consecutive sections of normal (F, I), CP (G, J), and PDAC (H, K) tissues is shown.

were normalized to the *β-actin* messenger RNA (mRNA) level, and the comparative 2–Ct method (2–deltaCT) was used for analysis.

Statistical Analysis

Graphs were created and statistical analyses were performed using the GraphPad Prism 4 Software (GraphPad, San Diego, CA). The percentages of CD31 and α-SMA staining and the results of ELISA and densitometric analyses are represented as mean ± SEM. The Mann-Whitney *U* test or Kruskal-Wallis and Dunn's multiple comparison tests were used for comparison of nonparametric data. The level of statistical significance was set at $P < .05$.

Results

Microvessel Density Decreases Significantly in the Diseased Pancreas

In the normal pancreas, there was a fine, homogenous blood supply to the parenchyma that was seen in the periacinar spaces. Both the scarce α-SMA positivity and the CD31 expression of the vessels were seen in the periacinar spaces (Figure 1, *A* and *B*, *arrows*). In CP and CP-like changes of the PDAC, periostin expression of PSCs preceded the expression of the typical activation marker (α-SMA) of PSCs (Figure 1, *C* and *D*, *arrows*). In the periacinar spaces, periostin staining colocalized with the fine capillary network detected by CD31 positivity (Figure 1*E*, *arrows*). In both CP and PDAC, the invading front of the activated stroma was marked by expansion of the periacinar spaces, where myofibroblasts deposited a periostin-rich ECM (Figure 2, *A* and *B*, *black arrows*). This maximal expression of periostin was not detected in organized fibrosis (Figure 2*A*, *white single-headed arrow*) or in the preserved parenchyma (Figure 2*A*, *white double-headed arrow*). As stromal invasion progressed into the parenchyma, the acini became gradually isolated, and tubular complexes started to appear (Figure 2*C*, *arrows*). These changes were also accompanied by a gradual decrease in the vascularity of the periacinar spaces as they became increasingly fibrotic. The MVD of the normal pancreas, as determined by CD31 expression, was five-fold and four-fold higher than in fibrotic areas of

CP ($P < .001$) and PDAC ($P < .01$), respectively (Figure 2*D*). The significant increase of α-SMA expression in fibrotic areas of CP (6.5-fold, $P < .05$) and PDAC (8.7-fold, $P < .01$) compared with that in the normal pancreas is depicted in Figure 2*E*. When CP and PDAC tissues were compared, the median MVD (+29%) and α-SMA (+33%) expressions of PDAC were higher than those of CP (not significant [n.s.]). In several peritumoral areas, the number of PSCs was higher than the number of PCCs (Figure 3*A*). The number of PSCs generally decreased in areas where thick bands of organized ECM proteins were deposited, but α-SMA and CD31 expression increased in a site-specific manner in the immediate peritumoral stroma (Figure 3, *B* and *C*, *arrows*). Similarly, in the immediate peritumoral stroma, increased periostin expression colocalized with the activated PSCs and irregular vessels (Figure 3, *D–F*).

Hypoxia Increases the Expression of α-SMA and Secretion of ECM Proteins in PSCs

The expected consequence of decreasing vascularity in the face of increasing fibrosis is hypoxia. Therefore, we analyzed PSCs' responses after 1 day (Figure 4*A*) and 3 days (Figure 4*B*) of hypoxia *in vitro*. Trypan blue staining was used to assess PSCs' viability after hypoxia. The combination of serum-free medium and hypoxia caused PSCs' death only after the fourth day (data not shown). Compared with the normoxic controls, 1 day of hypoxia slightly increased the α-SMA expression (122 ± 18%, n.s.) and approximately doubled the secretion of all ECM proteins: periostin (190 ± 61%, n.s.), type I collagen (230 ± 48%, n.s.), and fibronectin (206 ± 57%, n.s.). After 3 days of hypoxia, the expression of α-SMA significantly increased to 170 ± 34% ($P = .037$), and because of increased synthesis, secretion of periostin increased to 213 ± 82% ($P = .029$). In contrast, the synthesis of type I collagen and fibronectin was unchanged; thus, the secretion of type I collagen (95 ± 37%) and fibronectin (92 ± 42%) remained mostly unchanged compared with matching normoxic samples.

Regulation of VEGF and Endostatin Production of PCCs and PSCs under Hypoxia

Next, we assessed the effect of hypoxia on the secretion of angiogenic and antiangiogenic substances by PSCs and PCCs. ELISA was used to assess VEGF and endostatin secretion. Whereas hypoxic Panc-1 (198 ± 39%) and SU86.86 (597 ± 47%) SNs contained remarkably more VEGF than normoxic samples do, there was no obvious increase in the SNs of Colo-357 and MiaPaCa-2 cell lines. Importantly, PSCs were the most potent VEGF producers under hypoxia. With a 175 ± 124% increase under hypoxia compared with normoxic samples, they secreted more than double the amount of VEGF secreted by the most potent cancer cell (Figure 4*C*).

In contrast, hypoxia decreased endostatin secretion in both PCC and PSC SNs (Figure 4*D*). Importantly, MiaPaCa-2 and Panc-1 cell lines secreted more endostatin than PSCs (up to 15-fold) under normoxia. Although absolute values were reduced under hypoxia, MiaPaCa-2 and Panc-1 cell lines were also more potent than PSCs (up to 18-fold) in endostatin production.

Pancreatic Cancer Cell SNs Suppress Endothelial Cell Growth, Whereas Stellate Cell SNs Increase It

To test if VEGF and endostatin secretion of cultured PCCs and PSCs reflect their proangiogenic and antiangiogenic potencies *in vitro*,

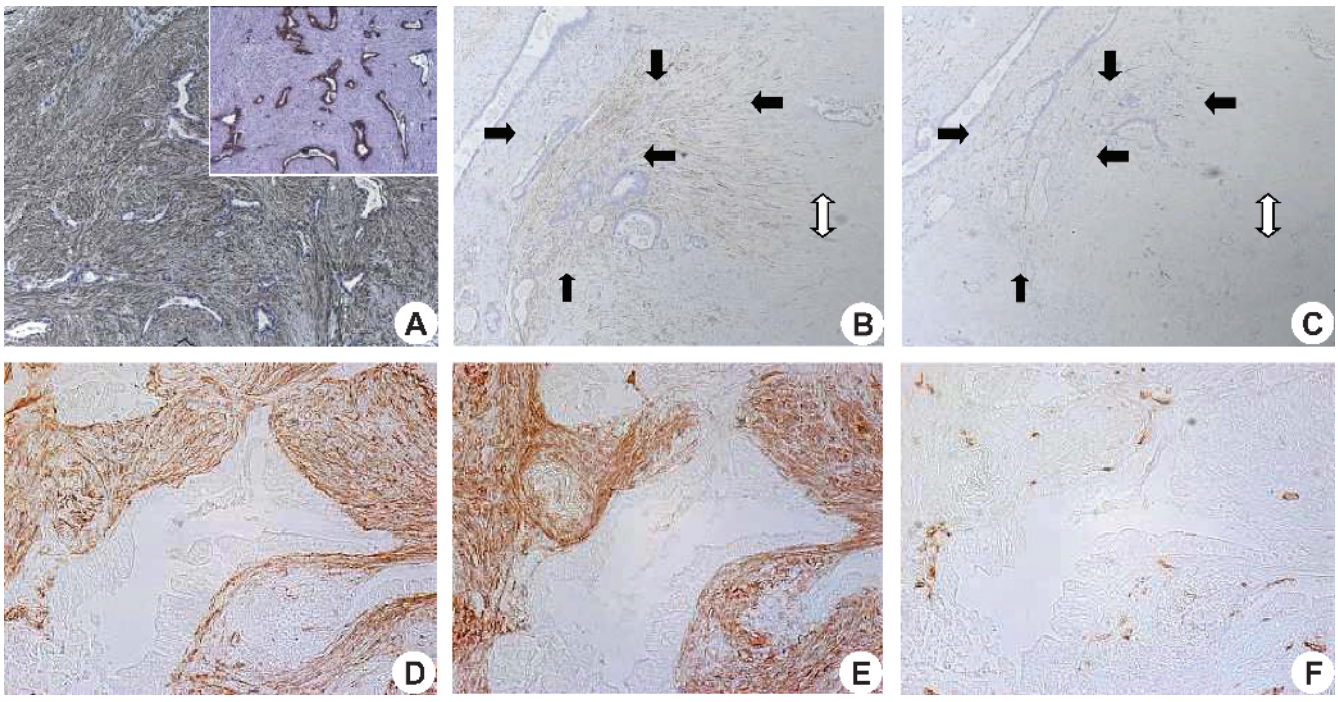

Figure 3. Analysis of peritumoral expression of α-SMA, periostin, and CD31: Immunohistochemical analysis on PDAC tissue was performed using anti–α-SMA antibody with hematoxylin counterstaining. Notice the significantly higher number of PSCs compared with cancer cells (A; original magnification, ×50). A demonstrative example of a highly desmoplastic PDAC is shown (B and C). Notice the mostly acellular ECM (white double arrow) and the increase in both α-SMA (B, black arrows) and CD31 (C, black arrows) staining in the peritumoral stroma. Colocalization of α-SMA (D; original magnification, ×100), periostin (E), and CD31 (F) around cancer structures is demonstrated in sections without counterstaining.

we treated HUVECs with the respective SNs. In accordance with the ELISA results, all PCC lines suppressed HUVECs' growth, by −25% to −92% compared with controls (Figure 5*A*). This suppression was consistently less prominent in hypoxic samples for all PCC lines (−9% to −59%). In contrast, PSCs increased the growth of HUVECs by up to 47%.

Effects of Pancreatic Cancer–Stellate Coculture on HUVECs' Growth

Because the SNs of monocellular cultures of PCCs and PSCs had opposite effects on HUVECs' growth, to simulate the *in vivo* situation, we assessed the effect of cancer and stellate cells' coculture SN on HUVECs' growth. For this purpose, the two highest endostatin-producing cancer cell lines (MiaPaCa-2 and Panc-1) were chosen for coculture experiments. Surprisingly, PSCs could not antagonize the antiangiogenic effects of PCCs; therefore, the coculture SNs were also predominantly antiangiogenic (Figure 5*B*).

Pancreatic Cancer and Stellate Cell Cocultures Increase Both VEGF and Endostatin Secretion

To elucidate the mechanism of the antiangiogenic effect of the coculture SN on HUVECs, we measured the VEGF and endostatin content of the common SN. Compared with the sum of the individual controls of PCCs and PSCs, the amount of VEGF secreted in the coculture SN was significantly higher ($P = .005$; Figure 6, *A* and *B*). Similarly, there was also a significant ($P = .002$) increase in endostatin in the coculture SN beyond the sum of the individual controls (Figure 6, *C* and *D*).

Cancer Cells Stimulate Stellate Cells to Secrete More VEGF, Whereas Stellate Cells Increase the Endostatin Production of Cancer Cells

To highlight the interaction between PCCs and PSCs, cells were cross-treated with each other's SNs. Compared with the sum of the individual controls, VEGF increased 390% if the stellate cells were treated with cancer cell SNs ($P < .001$), whereas endostatin increased 210% if the cancer cells were treated with PSC SNs ($P < .001$). When

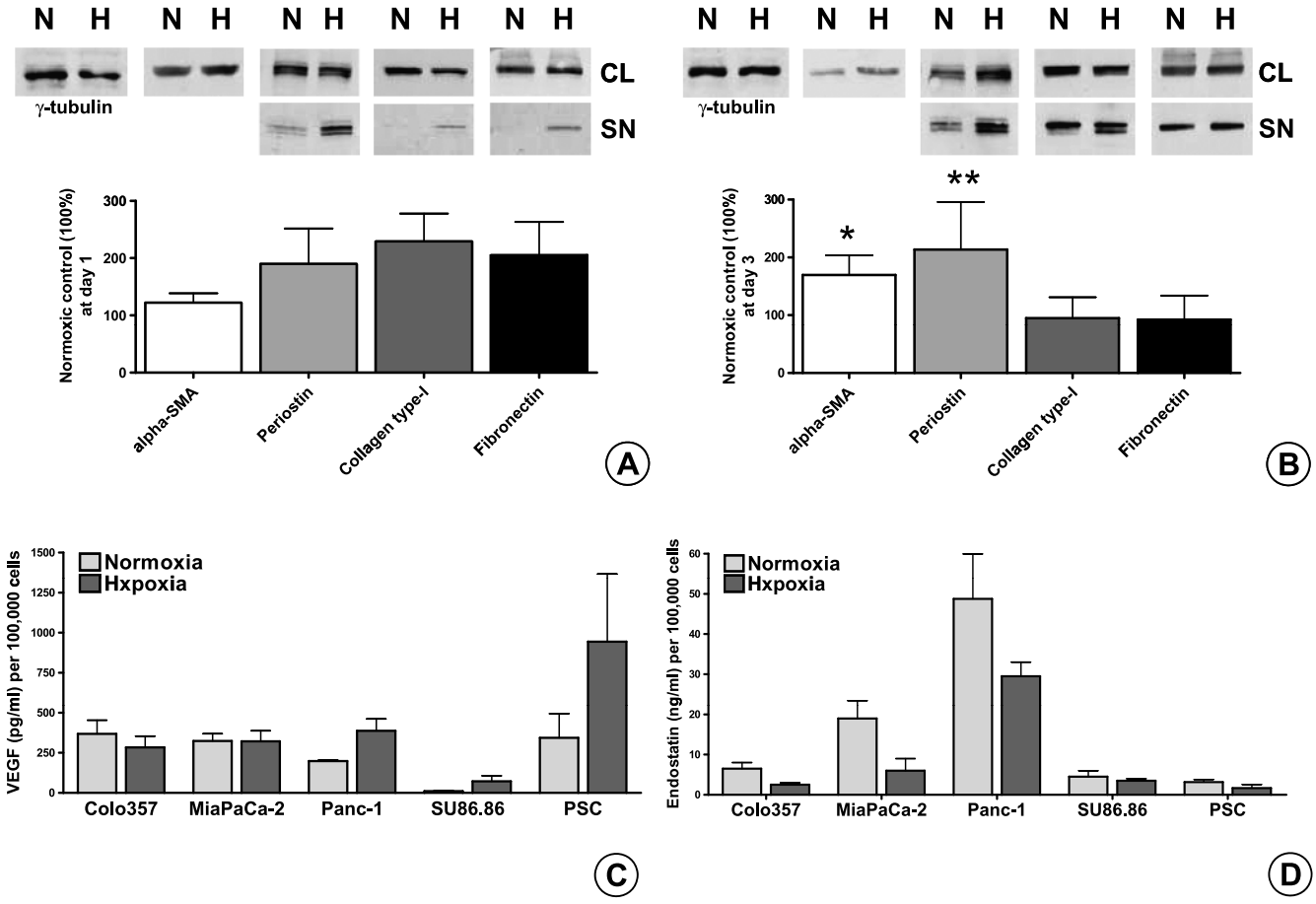

Figure 4. Effect of hypoxia on ECM protein synthesis and secretion of PSCs *in vitro* and quantification of secreted VEGF and endostatin in PCC and PSC SNs by ELISA: Sister clones of PSCs were kept under normoxic (N) and hypoxic (H) conditions for 1 (A) and 3 days (B) in serum-free medium. Matching CLs and SNs (SN) were analyzed by immunoblot analysis to evaluate the synthetic and secretory responses, respectively. All experiments were performed at least three times, and the results of densitometric analyses are presented as percent change (mean ± SEM) compared with the matching normoxic control (100%). Immunoblots were consecutively probed with α-SMA, periostin, type I collagen, fibronectin, and γ-tubulin antibodies. Sister clones of PCCs and PSCs were kept under normoxic and hypoxic conditions for 24 hours in serum-free medium. The amounts of VEGF (C) and endostatin (D) secreted in the SNs were quantified by ELISA. The values are expressed normalized to 100,000 cells. The experiments were performed at least three times using different PSC clones. *$P = .037$, **$P = .0286$.

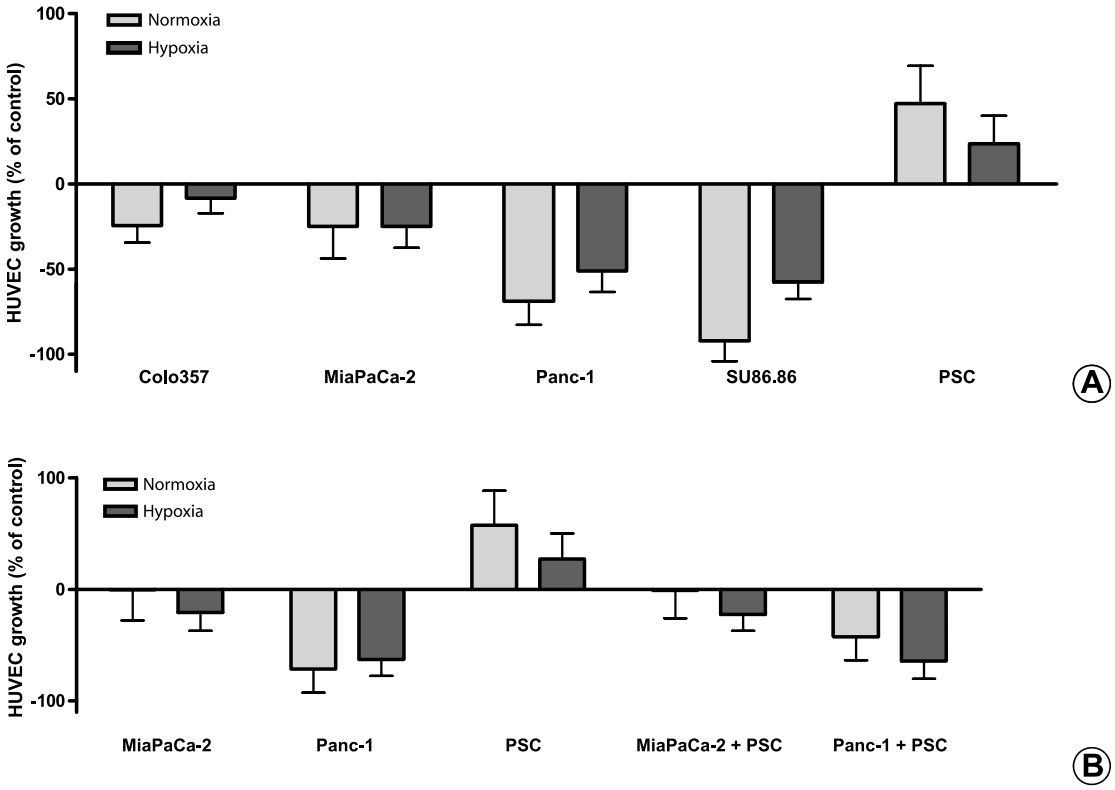

Figure 5. Assessment of HUVEC growth after treatment with PCC and PSC SNs: HUVECs were seeded in 96-well plates (5000 cells per well) in complete endothelial cell growth medium (100 μl per well). Twenty-four hours later, 100 μl of cancer cell or stellate cell or coculture SN was added to the cells. Forty-eight hours later, cell growth was assessed by MTT assay corrected for day 0. The experiments were performed at least nine times using three different HUVEC clones and three different PSC clones. The effect of four different cancer cell lines and PSC SNs on HUVEC growth is shown in panel (A). The effect of the common SN after coculture of MiaPaCa-2 and Panc-1 with PSC is shown in panel (B). The growth-inhibiting or growth-promoting effects of SNs on HUVECs are shown as percent change of the control (0%).

the sequence of treatment was reversed, the increase in VEGF and endostatin amounts was much less (65% and 26%, respectively) and did not reach statistical significance (Figure 7, *A* and *B*).

Increased Endostatin Production by Cancer Cells Is Not Due to Increased Synthesis

Because we showed before that PCCs can stimulate PSCs to secrete VEGF [22], we focused on how PSCs increase the endostatin production of cancer cells. When the amount of collagen XVIII mRNA (precursor of endostatin) was analyzed by quantitative real-time polymerase chain reaction, MiaPaCa-2 and Panc-1 had 5-fold and 43-fold higher relative mRNA ratios, respectively, compared with PSC. When the cancer cells were treated with PSC SNs, although there was no obvious increase in MiaPaCa-2 (–11 ± 26%), there was an 89 ± 50% increase of collagen XVIII mRNA in Panc-1 (data not shown). Because this cell line–specific (present in Panc-1 and absent in MiaPaCa-2) and modest increase did not explain the significant increase at the protein level observed in both cell lines, we evaluated whether the increase in endostatin was due to augmented cleavage from its precursor.

Both PCCs and PSCs Produce MMP-12 and Cathepsin B to Cleave Endostatin from Collagen XVIII

It is known that endostatin is cleaved from collagen XVIII by MMP-12 and cathepsins. Although both cancer cell lines secrete MMP-12, only 3 of 13 PSC clones secreted detectable amounts of MMP-12 (Figure 7*C*). There was also a slight increase of MMP-12 secreted in the SNs when PCCs and PSCs were cultured together (Figure 7*D*). Conversely, higher amounts of cathepsin B were produced by PSCs (Figure 7*E*).

Matrix Metalloproteinases Play a More Prominent Role in the Cleavage of Endostatin Than Cathepsins

Because no specific MMP-12 inhibitor is available, cells were treated with a broad-spectrum small-molecule MMP inhibitor that also inhibits MMP-12 activity. Similarly, a broad-spectrum small-molecule cathepsin inhibitor was used, which inhibits cathepsins B, S, and L. When the cancer cells were treated with the inhibitors, MMP inhibition resulted in a 65% reduction of endostatin production ($P < .001$), whereas cathepsin inhibition had no effect (Figure 8*A*). Because endostatin production by PSC was negligible, we tested the effect of the inhibitors when the PSCs were treated with cancer cell SNs. Matrix metalloproteinase inhibition resulted in a 49% reduction of endostatin production, whereas inhibition of cathepsins resulted in a 67% ($P < .001$) reduction of endostatin (Figure 8*B*). Next, we assessed the effect of the inhibitors during coculture of cancer and stellate cells. Compared with the sum of the controls, there was a 277 ± 36% increase in endostatin production in the common SN ($P < .001$). When the inhibitors were used, there was a 204% reduction by MMP inhibition ($P < .05$), whereas inhibition of cathepsin resulted only in a

24% reduction (Figure 8*C*). At the doses used in the experiments, neither drug had any negative effect on PSCs or PCCs growth (data not shown).

Discussion

Angiogenesis and ECM production are interrelated physiologic responses in wound healing and tissue regeneration, processes in which several molecules have bimodal functions. Recently, it has been reported that hypoxic induction of the key angiogenic molecule—VEGF—increased hepatic stellate cell activity, motility, and type I collagen synthesis [25]. Like their counterparts in the liver, PSCs also have strong proangiogenic attributes through secretion of VEGF, basic fibroblast growth factor, periostin, and type I collagen [3,4,22,26,27]. Periostin, which is known to induce angiogenesis in colon and breast cancers, is uniquely secreted by PSCs in the pancreas [4,26,27]. Like type I collagen, periostin promotes endothelial cell growth and motility and perpetuates the fibrogenic activity of PSCs [4,26,27].

Unlike in acute pancreatitis, where PSCs' activity is transient, PSCs of the CP and pancreatic cancer–associated stroma maintain their activated phenotype and secrete excessive amounts of ECM proteins, leading to organ fibrosis and hypoxia [4,21,24,28,29]. *In vitro*, hypoxia strongly induces both periostin and VEGF secretion while suppressing endostatin production of PSCs. As expected, PSCs promote endothelial cell growth under both normoxic and hypoxic conditions.

What remains paradoxical is why both CP and PDAC are hypovascular and therefore hypoxic compared with normal tissues [21]. It seems likely that abnormal deposition of the stromal proteins by PSCs in CP and PDAC distorts the normal parencyhmal architecture and interferes with oxygen diffusion into the tissues. We have previously shown that there is very scarce expression of periostin in the normal pancreas, but once activated by cancer cells, PSCs remain fibrogenic and secrete abundant type I collagen and fibronectin because of an autocrine-positive feedback loop running over periostin [4]. We now show that: 1) although it is less than that in cancer, there is also a remarkable increase of periostin in CP compared with that in the normal pancreas; 2) this highly site-specific periostin overexpression is found in the periacinar spaces on the invading front of the activated stroma, where acini are isolated by abnormal deposition of ECM proteins; 3) hypoxia increases PSCs' activity as well as secretion of periostin, type I collagen, and fibronectin; and 4) because periostin expression of PSCs precedes α-SMA expression, it may be used as an early activation marker for PSCs *in vivo*, as they transform from quiescent PSCs into activated myofibroblasts. Viewed in combination, these observations may explain why CP-like changes in PDAC progress ahead and beyond of cancer cells [13,24].

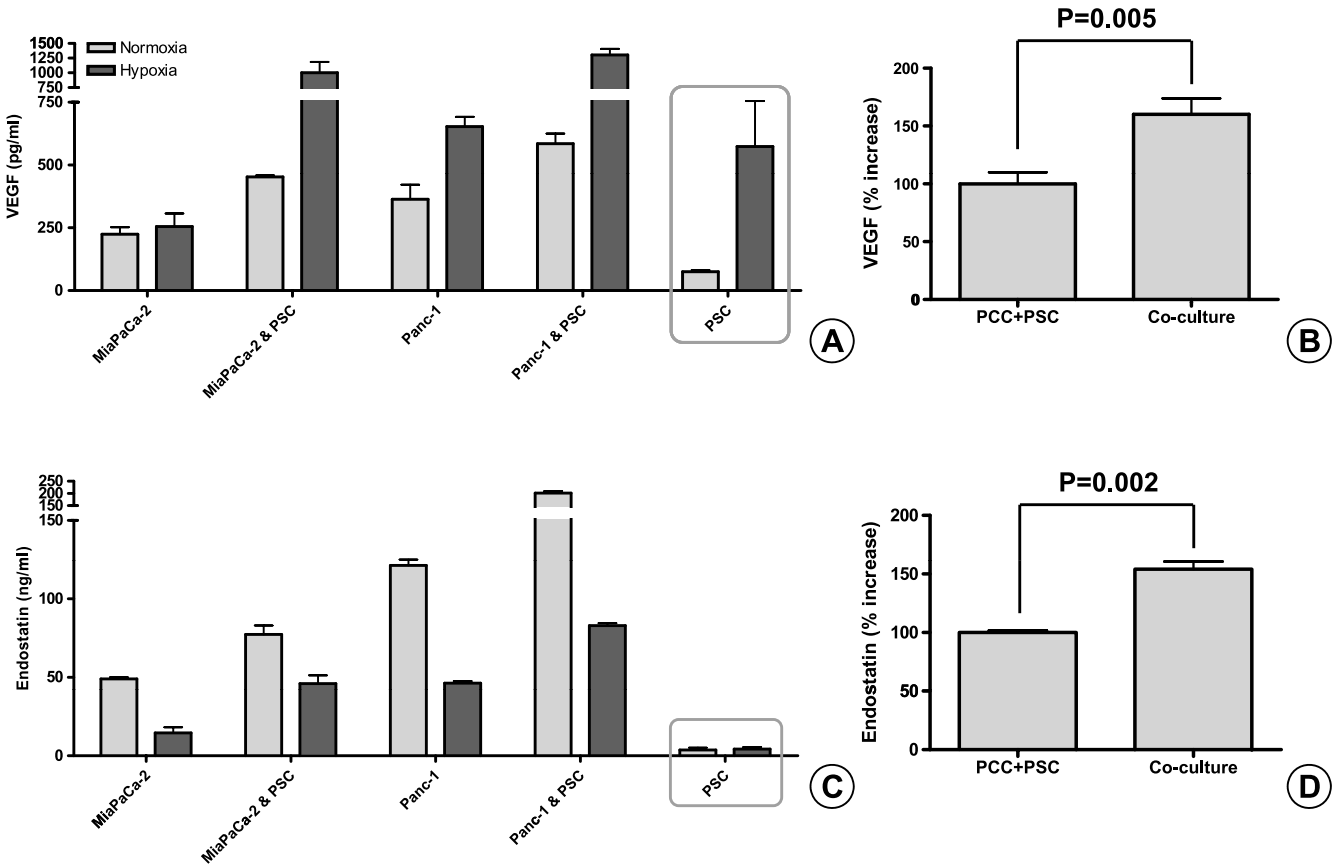

Figure 6. Quantification of VEGF and endostatin secretion in pancreatic cancer–stellate cell coculture SNs by ELISA: PSC (200,000 cells per well) and PCC (400,000 cells per insert, 1-μm pore size) were cocultured for 24 hours in serum-free medium. The amount of VEGF (A) and endostatin (C) secreted in the common SN was quantified by ELISA. The experiments were repeated at least twice using different PSC clones. In comparison to the mathematical sum of the individual controls (PCC + PSC), the increase of VEGF (B) and endostatin (D) in the common SN after coculture of MiaPaCa-2 and Panc-1 with PSCs is expressed in percentages.

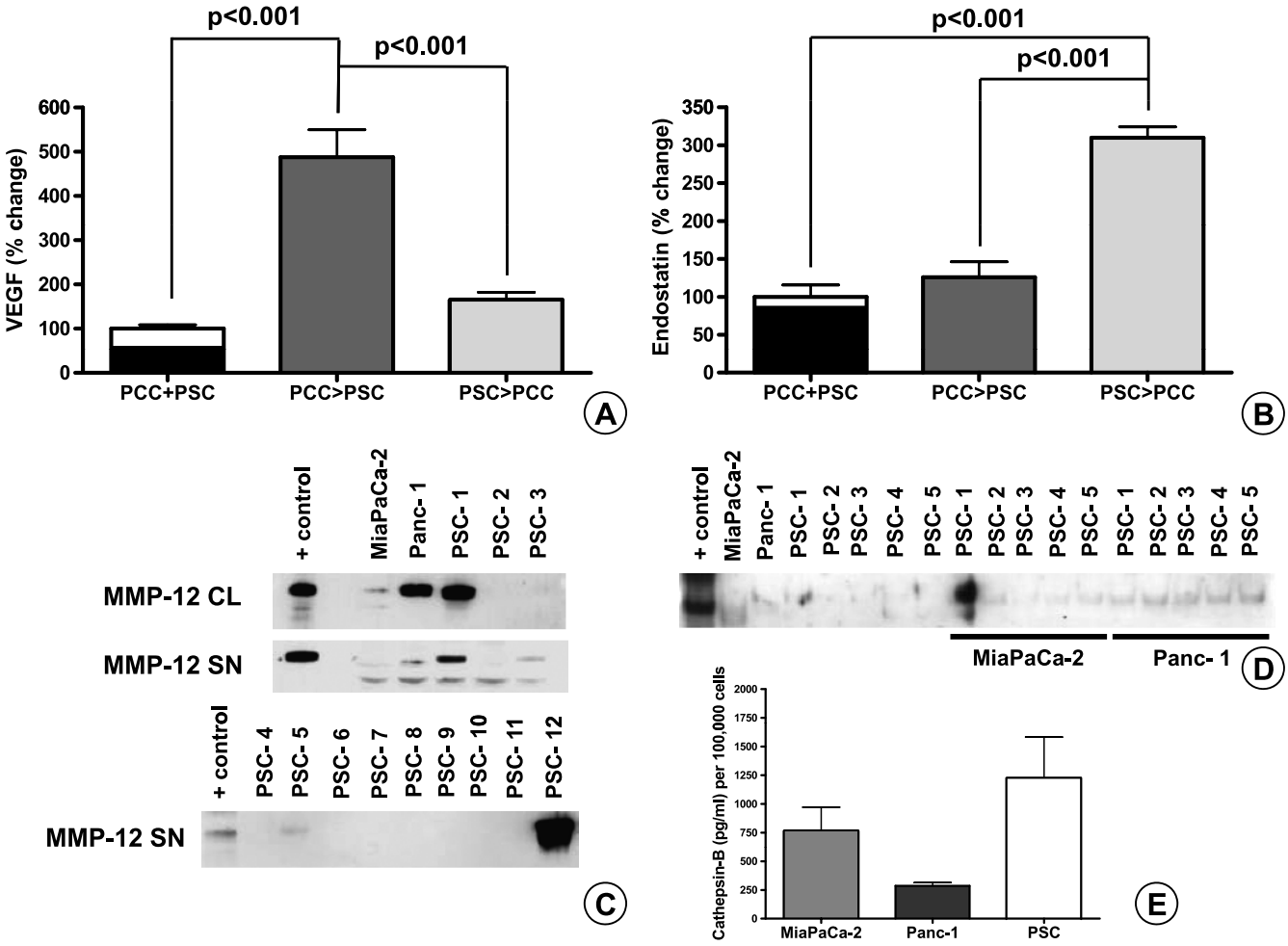

Figure 7. Quantification of secreted VEGF and endostatin by ELISA after exchange of SNs between PSCs and PCCs and assessment of MMP-12 and cathepsin B production by PSCs and PCCs: PSC (200,000 cells per well) and PCC (400,000 cells per well) were cultured in serum-free medium. After 24 hours, the individual SNs were exchanged and kept on the reciprocal cells for another day. PCC > PSC denotes cancer cell SN added to PSC; PSC > PCC denotes PSC SN added to cancer cells. In the control wells, serum-free medium was used to incubate the cells for 24 hours. The amount of VEGF (A) and endostatin (B) secreted was quantified by ELISA. In the control columns (PCC + PSC), the VEGF and endostatin produced by PCCs in 24 hours (black column) are mathematically added to the amount produced by the PSCs (white column above the black). The experiments were repeated three times using different PSC clones. Immunoblot analysis was used to measure the MMP-12 in the CLs and in the SN of cells (C). Five nanograms of MMP-12 was loaded to the first column as positive control (AG902; Millipore). MMP-12 secreted by cocultured PCC and PSC is shown (D). Secreted cathepsin B was quantified by ELISA (E). Error bars, SEM.

Within the confines of a fibrotic tumor stroma, capillary perfusion decreases as tissue pressure increases, because of the increasing number of cancer cells [15,30,31]. Similarly, secondary to excessive PSCs' growth and ECM deposition, the capillaries are probably compressed, hindering blood perfusion of the normal pancreas. Therefore, on the invasive front of the activated stroma, continuous activation of PSCs in the periacinar spaces and the subsequent deposition of ECM proteins around a fine capillary network may physically cause tissue hypoxia by hindering the blood circulation and oxygen diffusion. In line with this argument, PSCs' activity (α-SMA, periostin) increased significantly in the diseased pancreas, with excessive deposition of ECM in the periacinar spaces, whereas MVD decreased reciprocally.

It is becoming clearer that tumors grow by co-opting their neighboring stromal cells and host vessels, which then provide the tumors with environmental and vascular support [4,10,19,32]. According to Yancopoulos et al. [10], in response to tumor co-option, the host vessels mount a defensive response. Sensing inappropriate co-option, they regress, which results in a secondarily avascular and hypoxic tumor [10].

In our study, as demonstrated in the literature, organ fibrosis (CP) was associated with a rarefication of the microvasculature [15]. In contrast, however, although solid tumors are known to be typically more vascularized than normal tissues [7,19], PDAC is a hypovascular and hypoxic tumor. One possible explanation is that PCCs produce remarkable amounts of endostatin, *in vitro* and *in vivo*, even under hypoxia. Endostatin is a 20-kDa C-terminal fragment of collagen XVIII that specifically inhibits endothelial proliferation and potently inhibits angiogenesis [28]. It is cleaved from its precursor by MMP-12 and cathepsins such as B and L [33–35]. We have previously shown by IHC that PDAC cells and peritumoral stromal cells express MMP-12 [36]. Now, we show that PSCs modulate endostatin production of PCCs mostly by cleaving endostatin from its precursor. When PSCs were cocultured with PCCs or when PSC SN was used to incubate, there was

an increase in the final endostatin amount, as it was mainly produced by PCCs (without a concomitant rise in collagen XVIII mRNA expression) through cleavage of collagen XVIII by PSC- and PCC-derived MMP-12. This is in line with our and with other groups' previous observations that cancer cells induce MMP production of PSCs around them [36].

Nonetheless, in comparison to CP tissues, PDAC tissues expressed 33% more α-SMA and had a 29% higher MVD, although these differences were statistically not significant when the overall expressions were compared. The changes were mostly seen in the immediate peritumoral reactive stroma, where a consistent increase beyond their overall expression was found in α-SMA, periostin, and CD31 staining. Therefore, several lines of evidence suggest that PDAC at least partially induces neoangiogenesis by co-opting PSCs: 1) periostin is a proangiogenic molecule secreted by PSCs [4,26,27]; 2) PCCs activate PSCs and increase their periostin production [3,4]; 3) under hypoxia, activated PSCs secrete higher amounts of VEGF than the cancer cells do; 4) PCC SNs suppress HUVECs' growth, whereas PSC SNs promote it; and 5) the disorganized tumor vessels are not seen in the fibrotic part of the stroma but mostly in the reactive stroma around the cancer cells. Probably, PCCs co-opt PSCs by initially creating local hypoxia with their antiangiogenic attributes. In response to hypoxia, both cancer cells and activated stellate cells then produce excessive VEGF, creating a locally proangiogenic microenvironment that facilitates endothelial cell recruitment mostly in the immediate vicinity of the cancer cells. Nevertheless, the same inducers of angiogenic PSC responses (activation by cancer, hypoxia) also elicit a stronger fibrogenic response which ultimately creates a fibrotic/hypoxic tissue (Figure 9).

Stellate cells augment pancreatic tumor development and possibly increase their metastatic spread in animal models [3,32,37]. It is still

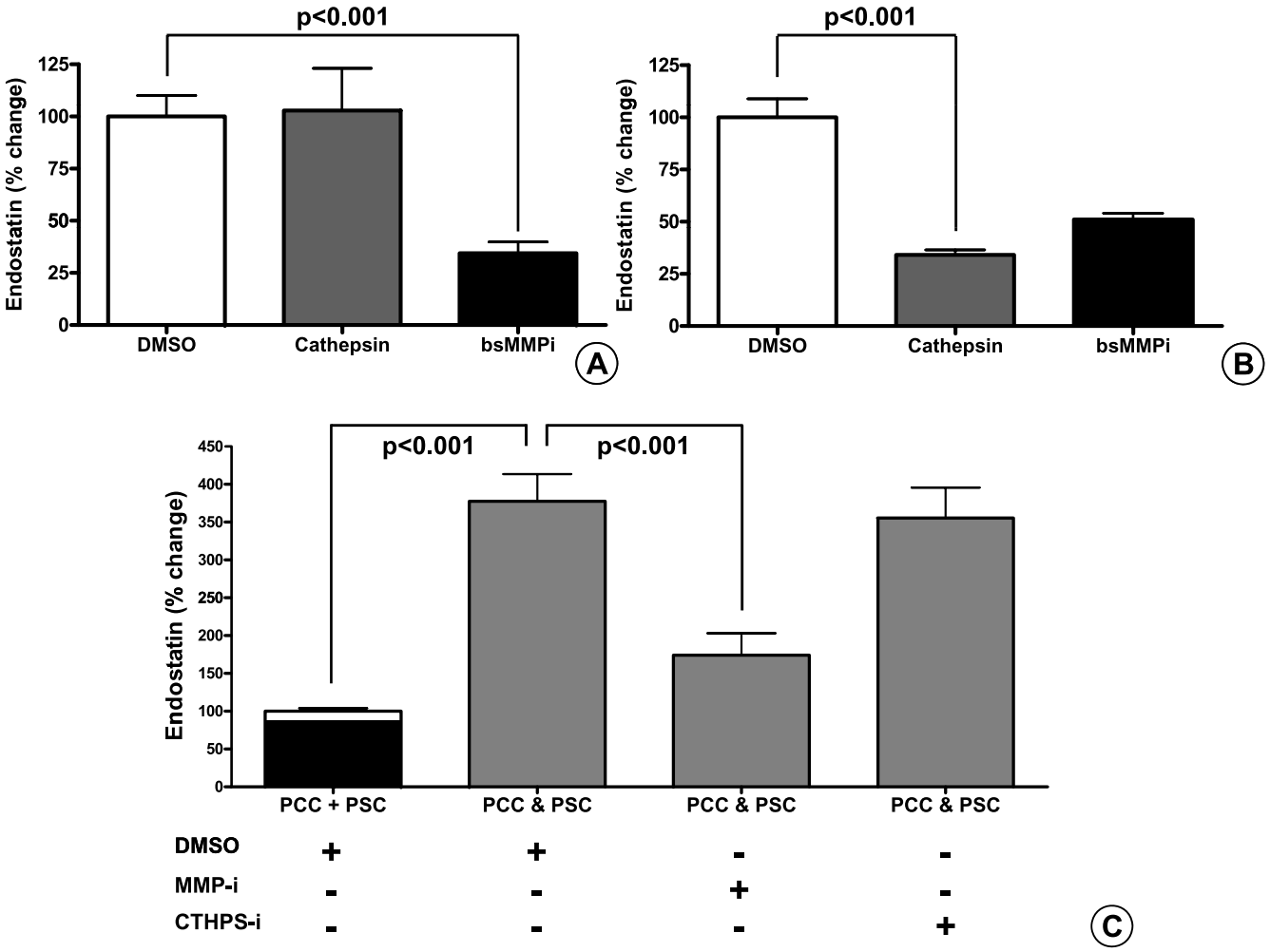

Figure 8. Quantification of secreted endostatin by ELISA after treatment with small-molecule broad-spectrum inhibitors of MMP and cathepsin: MiaPaCa-2 and Panc-1 (400,000 cells per well) were cultured alone (A) or cocultured with PSCs (C) for 24 hours in the presence of a small-molecule broad-spectrum MMP inhibitor (50 μM), cathepsin inhibitor (10 μM), or DMSO as control. To assess their effect on the cleavage of endostatin from the secreted collagen XVIII by cancer cells, inhibitors were added to the cancer cell SNs that were used to incubate PSC (200,000 cells per well) for 24 hours (B). Changes are expressed as percentages compared with the appropriate control (sum of the DMSO controls of PCC and PSC: PCC + PSC, 100%). PCC & PSC denotes the coculture of PCC and PSC in the presence of DMSO (control), small-molecule broad-spectrum MMP inhibitor (50 μM), or cathepsin inhibitor (10 μM). Error bars show the SEM. The experiments were repeated using five different PSC clones and two different cancer cell lines. The amount of endostatin secreted was quantified by ELISA.

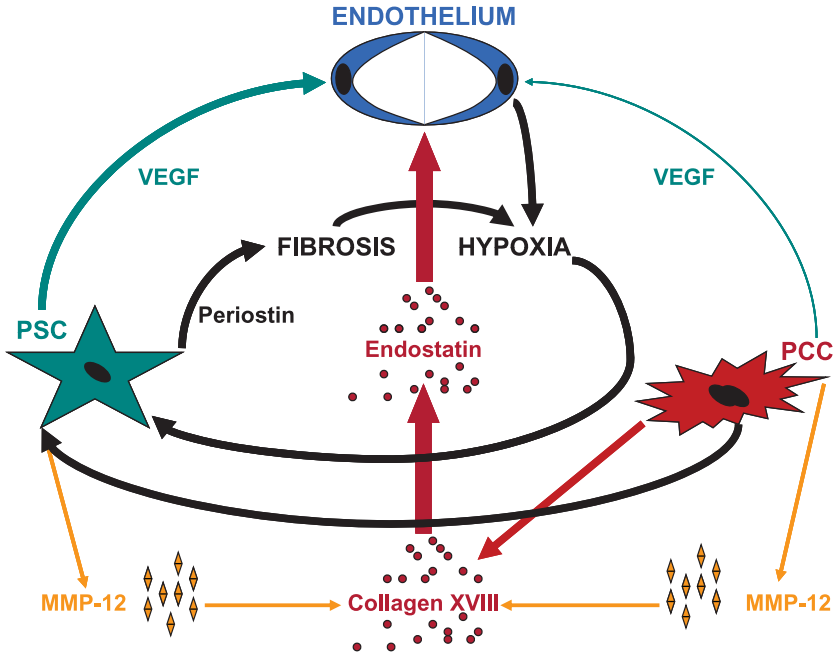

Figure 9. Schematic representation of the combined effects of cancer–stellate cell system on endothelial cells.

unknown by which mechanisms PSCs contribute to this excessive tumor growth and dissemination. One possible explanation could be increased angiogenesis. Here, we used VEGF and endostatin as surrogate markers for proangiogenic and antiangiogenic attributes of PSCs and PCCs. Nevertheless, it would be an oversimplification to reduce neoangiogenesis to a balance between VEGF and endostatin only and disregard several other proangiogenic and antiangiogenic factors known to be secreted by cancer cells, stellate cells, and inflammatory cells. For example, the SNs of the PSCs obtained under normoxic conditions (which contain less VEGF and more endostatin) increased HUVECs' growth more than the hypoxic ones. Although statistically insignificant, this unexpected effect underlines the presence of other possible factors affecting HUVECs' growth and needs further clarification.

In conclusion, PDAC is an extremely scirrhous and hypoxic tumor due to both fibrogenic effects of PSCs and antiangiogenic effects of cancer cells. Pancreatic stellate cells can produce remarkable amounts of VEGF and modulate the amount of endostatin produced by cancer cells. Therefore, in contrast to expectations, localized increase of MVD around cancer structures is not a function of cancer cells but is probably a result of the proangiogenic attributes of peritumoral PSCs. Nonetheless, deposition of excessive ECM proteins in the periacinar spaces and perpetuation of PSCs' activity under hypoxia overwhelms PSCs' local proangiogenic properties, creating tissue hypoxia in CP and pancreatic cancer (Figure 9). These findings may help explain why antiangiogenic therapies generally fail in PDAC and suggest that novel therapeutic approaches targeting cancer-stroma interactions could be explored [23].

References

[1] Erkan M, Michalski CW, Rieder S, Reiser-Erkan C, Abiatari I, Kolb A, Giese NA, Esposito I, Friess H, and Kleeff J (2008). The activated stroma index is a novel and independent prognostic marker in pancreatic ductal adenocarcinoma. *Clin Gastroenterol Hepatol* **6** (10), 1155–1161.

[2] Apte MV, Haber PS, Darby SJ, Rodgers SC, McCaughan GW, Korsten MA, Pirola RC, and Wilson JS (1999). Pancreatic stellate cells are activated by proinflammatory cytokines: implications for pancreatic fibrogenesis. *Gut* **44**, 534–541.

[3] Bachem MG, Schunemann M, Ramadani M, Siech M, Beger H, Buck A, Zhou S, Schmid-Kotsas A, and Adler G (2005). Pancreatic carcinoma cells induce fibrosis by stimulating proliferation and matrix synthesis of stellate cells. *Gastroenterology* **128**, 907–921.

[4] Erkan M, Kleeff J, Gorbachevski A, Reiser C, Mitkus T, Esposito I, Giese T, Buchler MW, Giese NA, and Friess H (2007). Periostin creates a tumor-supportive microenvironment in the pancreas by sustaining fibrogenic stellate cell activity. *Gastroenterology* **132**, 1447–1464.

[5] Reiser-Erkan C, Erkan M, Pan Z, Bekasi S, Giese NA, Streit S, Michalski CW, Friess H, and Kleeff J (2008). Hypoxia-inducible proto-oncogene *Pim-1* is a prognostic marker in pancreatic ductal adenocarcinoma. *Cancer Biol Ther* **7**, 1352–1359.

[6] Folkman J (2006). Angiogenesis. *Annu Rev Med* **57**, 1–18.

[7] Folkman J, Watson K, Ingber D, and Hanahan D (1989). Induction of angiogenesis during the transition from hyperplasia to neoplasia. *Nature* **339**, 58–61.

[8] Hori A, Sasada R, Matsutani E, Naito K, Sakura Y, Fujita T, and Kozai Y (1991). Suppression of solid tumor growth by immunoneutralizing monoclonal antibody against human basic fibroblast growth factor. *Cancer Res* **51**, 6180–6184.

[9] Hanahan D and Weinberg RA (2000). The hallmarks of cancer. *Cell* **100**, 57–70.

[10] Yancopoulos GD, Davis S, Gale NW, Rudge JS, Wiegand SJ, and Holash J (2000). Vascular-specific growth factors and blood vessel formation. *Nature* **407**, 242–248.

[11] Carmeliet P (2003). Angiogenesis in health and disease. *Nat Med* **9**, 653–660.

[12] Abdollahi A, Schwager C, Kleeff J, Esposito I, Domhan S, Peschke P, Hauser K, Hahnfeldt P, Hlatky L, Debus J, et al. (2007). Transcriptional network governing the angiogenic switch in human pancreatic cancer. *Proc Natl Acad Sci USA* **104**, 12890–12895.

[13] Bissell MJ and Radisky D (2001). Putting tumours in context. *Nat Rev Cancer* **1**, 46–54.

[14] Holash J, Maisonpierre PC, Compton D, Boland P, Alexander CR, Zagzag D, Yancopoulos GD, and Wiegand SJ (1999). Vessel cooption, regression, and growth in tumors mediated by angiopoietins and VEGF. *Science* **284**, 1994–1998.

[15] Brown LF, Dvorak AM, and Dvorak HF (1989). Leaky vessels, fibrin deposition, and fibrosis: a sequence of events common to solid tumors and to many other types of disease. *Am Rev Respir Dis* **140**, 1104–1107.

[16] Brown LF, Guidi AJ, Schnitt SJ, Van De Water L, Iruela-Arispe ML, Yeo TK, Tognazzi K, and Dvorak HF (1999). Vascular stroma formation in carcinoma *in situ*, invasive carcinoma, and metastatic carcinoma of the breast. *Clin Cancer Res* **5**, 1041–1056.

[17] Leung DW, Cachianes G, Kuang WJ, Goeddel DV, and Ferrara N (1989). Vascular endothelial growth factor is a secreted angiogenic mitogen. *Science* **246**, 1306–1309.
[18] Masamune A, Kikuta K, Watanabe T, Satoh K, Hirota M, and Shimosegawa T (2008). Hypoxia stimulates pancreatic stellate cells to induce fibrosis and angiogenesis in pancreatic cancer. *Am J Physiol Gastrointest Liver Physiol* **295** (4), G709–G717.
[19] Kalluri R and Zeisberg M (2006). Fibroblasts in cancer. *Nat Rev Cancer* **6**, 392–401.
[20] Fukumura D, Xavier R, Sugiura T, Chen Y, Park EC, Lu N, Selig M, Nielsen G, Taksir T, Jain RK, et al. (1998). Tumor induction of VEGF promoter activity in stromal cells. *Cell* **94**, 715–725.
[21] Couvelard A, O'Toole D, Leek R, Turley H, Sauvanet A, Degott C, Ruszniewski P, Belghiti J, Harris AL, Gatter K, et al. (2005). Expression of hypoxia-inducible factors is correlated with the presence of a fibrotic focus and angiogenesis in pancreatic ductal adenocarcinomas. *Histopathology* **46**, 668–676.
[22] Zhang W, Erkan M, Abiatari I, Giese NA, Felix K, Kayed H, Buchler MW, Friess H, and Kleeff J (2007). Expression of extracellular matrix metalloproteinase inducer (EMMPRIN/CD147) in pancreatic neoplasm and pancreatic stellate cells. *Cancer Biol Ther* **6**, 218–227.
[23] Kindler HL, Niedzwiecki D, Hollis D, Oraefo E, Schrag D, Hurwitz H, McLeod HL, Mulcahy MF, Schilsky RL, Goldberg RM, and Cancer and Leukemia Group B (2007). Gemcitabine plus bevacizumab no better than gemcitabine alone in clinical study of 600 patients with pancreatic cancer. *Cancer Biol Ther* **6**, 137.
[24] Erkan M, Kleeff J, Esposito I, Giese T, Ketterer K, Buchler MW, Giese NA, and Friess H (2005). Loss of BNIP3 expression is a late event in pancreatic cancer contributing to chemoresistance and worsened prognosis. *Oncogene* **24**, 4421–4432.
[25] Novo E, Cannito S, Zamara E, Valfre di Bonzo L, Caligiuri A, Cravanzola C, Compagnone A, Colombatto S, Marra F, Pinzani M, et al. (2007). Proangiogenic cytokines as hypoxia-dependent factors stimulating migration of human hepatic stellate cells. *Am J Pathol* **170**, 1942–1953.
[26] Bao S, Ouyang G, Bai X, Huang Z, Ma C, Liu M, Shao R, Anderson RM, Rich JN, and Wang XF (2004). Periostin potently promotes metastatic growth of colon cancer by augmenting cell survival via the Akt/PKB pathway. *Cancer Cell* **5**, 329–339.
[27] Shao R, Bao S, Bai X, Blanchette C, Anderson RM, Dang T, Gishizky ML, Marks JR, and Wang XF (2004). Acquired expression of periostin by human breast cancers promotes tumor angiogenesis through up-regulation of vascular endothelial growth factor receptor 2 expression. *Mol Cell Biol* **24**, 3992–4003.
[28] O'Reilly MS, Boehm T, Shing Y, Fukai N, Vasios G, Lane WS, Flynn E, Birkhead JR, Olsen BR, and Folkman J (1997). Endostatin: an endogenous inhibitor of angiogenesis and tumor growth. *Cell* **88**, 277–285.
[29] Schneiderhan W, Diaz F, Fundel M, Zhou S, Siech M, Hasel C, Moller P, Gschwend JE, Seufferlein T, Gress T, et al. (2007). Pancreatic stellate cells are an important source of MMP-2 in human pancreatic cancer and accelerate tumor progression in a murine xenograft model and CAM assay. *J Cell Sci* **120**, 512–519.
[30] Boucher Y, Leunig M, and Jain RK (1996). Tumor angiogenesis and interstitial hypertension. *Cancer Res* **56**, 4264–4266.
[31] Kozin SV, Winkler F, Garkavtsev I, Hicklin DJ, Jain RK, and Boucher Y (2007). Human tumor xenografts recurring after radiotherapy are more sensitive to anti–vascular endothelial growth factor receptor-2 treatment than treatment-naive tumors. *Cancer Res* **67**, 5076–5082.
[32] Vonlaufen A, Joshi S, Qu C, Phillips PA, Xu Z, Parker NR, Toi CS, Pirola RC, Wilson JS, Goldstein D, et al. (2008). Pancreatic stellate cells: partners in crime with pancreatic cancer cells. *Cancer Res* **68**, 2085–2093.
[33] Brammer RD, Bramhall SR, and Eggo MC (2005). Endostatin expression in pancreatic tissue is modulated by elastase. *Br J Cancer* **92**, 89–93.
[34] Ferreras M, Felbor U, Lenhard T, Olsen BR, and Delaisse J (2000). Generation and degradation of human endostatin proteins by various proteinases. *FEBS Lett* **486**, 247–251.
[35] Im E, Venkatakrishnan A, and Kazlauskas A (2005). Cathepsin B regulates the intrinsic angiogenic threshold of endothelial cells. *Mol Biol Cell* **16**, 3488–3500.
[36] Balaz P, Friess H, Kondo Y, Zhu Z, Zimmermann A, and Buchler MW (2002). Human macrophage metalloelastase worsens the prognosis of pancreatic cancer. *Ann Surg* **235**, 519–527.
[37] Hwang RF, Moore T, Arumugam T, Ramachandran V, Amos KD, Rivera A, Ji B, Evans DB, and Logsdon CD (2008). Cancer-associated stromal fibroblasts promote pancreatic tumor progression. *Cancer Res* **68**, 918–926.